Materials Science & Engineering A 559 (2013) 601–606

Contents lists available at SciVerse ScienceDirect

Materials Science & Engineering A

journal homepage: www.elsevier.com/locate/msea

Homogenization of ECAPed Al 2024 alloy through age-hardening

G. Kotan [a,b,*], E. Tan [a], Y.E. Kalay [a], C.H. Gür [a]

[a] Department of Metallurgical and Materials Engineering, Middle East Technical University, Ankara, Turkey
[b] Department of Metallurgical and Materials Engineering, Mersin University, Içel, Turkey

ARTICLE INFO

Article history:
Received 7 July 2012
Received in revised form
29 August 2012
Accepted 30 August 2012
Available online 5 September 2012

Keywords:
Aluminium alloy
Equal channel angular pressing
Aging
Microstructure
Homogeneity

ABSTRACT

Mechanical properties of aluminum alloys can be improved by obtaining ultra-fine grained structures via severe plastic deformation methods such as equal channel angular pressing (ECAP). In practice, however, the final structure may not be as homogeneous as desired. Thus, elimination of the inhomogeneity of ECAPed samples is a challenging task. In the case of age-hardenable alloys, a combination of ECAP and aging might provide new means of obtaining microstructural homogeneity. In this study, the effect of post-ECAP aging on the microstructural homogeneity of 2024 Al–Cu–Mg alloy was investigated. Following solutionization and rapid cooling, some samples were aged at 190 °C for various times. Another group of samples were similarly aged after one-pass ECAP through a 120° die. Throughout the aging of the samples, maps of microhardness variation were acquired in order to monitor the precipitation behavior. It was observed that considerable homogenization in the microstructure of the ECAPed samples was reached, especially right after peak aging. The homogenization level was characterized with the hardness inhomogeneity index. EBSD and TEM investigations were performed to observe variations in the homogeneity of the microstructure.

1. Introduction

Al alloys are classified as light-weight, high strength materials [1]; however their mechanical properties still need to be improved to be used in critical applications. Al 2024 is a high-strength, age-hardenable Al–Cu–Mg alloy, and it is widely used in the aerospace and transport industries [1,2]. Age-hardening is one of the well-known techniques used to improve the mechanical properties of this alloy by providing a nearly 50% hardness increment [3]. On the other hand, a relatively new approach is to combine cold working with age-hardening to attain further strengthening and homogenization of the structure [4]. The main disadvantage of cold working is the undesirable change in the size and shape of the material, which often causes stress related cracking. For instance, in both sheet and rod production there is a deformation limit to preserve crack-free structures; as a result, multiple passes are obligatory to achieve remarkable strength [4].

Severe plastic deformation (SPD), an alternative technique to classical deformation hardening methods, aims to obtain ultra-fine grain structure, lower than 1 μm, with high angle grain boundaries uniformly distributed throughout the volume, free from the cracks or damage [5]. Among the SPD techniques, equal channel angular pressing (ECAP) and high pressure torsion (HPT) are the most promising. ECAP is comparatively simple and easy to perform on various alloys and composites. It is applicable to large billets and provides complete homogeneity in the final product [6]. ECAP can be used for samples as large as 4 cm in diameter and 10 cm in length [7]. In contrast, by HPT, the sample size limitation is so dominant that an exceedingly ductile Al sample of 8.57 mm in height and 10 mm in diameter could be hardly produced [8]. In the case of Al 2024 alloy, production was limited to 1.5 mm in thickness and 14 mm in diameter; a hardness value of 275 HV was attainable [9].

In practice, however, the final structure after the ECAP process may not be as homogeneous as desired. There are several studies on the elimination of this inhomogeneity through annealing [10] or further ECAP processing [11]. Finite element analyses in ECAP have shown that the lower part of the sample has less strain [12,13], which results in inhomogeneity in both the microstructure and mechanical properties of the sample. Usually homogenization in ECAP is achieved by increasing the number of passes, but even this treatment does not always result in total elimination of inhomogeneity. For instance, ECAP processing of age-hardenable Al alloys of 2024 and 6061 has resulted in a minimum hardness deviation ($\Delta H = H_{maximum} - H_{minimum}$) of 15 HV after 6 passes. In fact, for some regions the difference becomes as high as 30 HV [11]. In another study, the ECAP carried out inside a copper tube led to a very low ΔHV of 4 HV for pure Al after four passes [14]. As these previous studies indicate, there is still no

* Corresponding author at: Middle East Technical University, Department of Metallurgical and Materials Engineering, METU Universiteler Mah. Dumlupınar Blv. No:1, 06800 Ankara, Turkey. Tel.: +90 312 210 5924; fax: +90 312 210 2518.
E-mail addresses: guher@metu.edu.tr, guherkotan@gmail.com (G. Kotan).

0921-5093/$ - see front matter © 2012 Elsevier B.V. All rights reserved.
http://dx.doi.org/10.1016/j.msea.2012.08.148

agreement on the degree of homogeneity after ECAP; further studies are necessary to reveal this relationship.

In the FEM analysis studies inhomogeneity was defined using a parameter, called strain inhomogeneity index, which is:

$$\varepsilon_i = \frac{(\varepsilon_{max} - \varepsilon_{min})}{\varepsilon_{avg}} \quad (1)$$

where ε_{max}, $\varepsilon_{min,}$ and ε_{avg} are maximum, minimum, and average magnitudes of effective strain [14,15]. With a similar approach, a hardness inhomogeneity index can be defined as:

$$H_i = \frac{(H_{max} - H_{min})}{H_{avg}} \quad (2)$$

where H_{max}, H_{min} and H_{avg} represent maximum, minimum, and average hardness values, respectively. In this manner, both average values and hardness variations are included in the data analysis. The range of deviation is an important index as it remarks weaker regions that may act as fracture initiation sites.

The deformation inhomogeneity manifested in the first pass diminishes after an adequate number of ECAP passes, to a certain extent. Ultra-fine grain structure can only be achieved after some definite number of passes, but the minimum grain size achievable is said to be dependent mainly on the amount of strain induced after the first pass. The first ECAP pass has the most significant impact on mechanical properties and final grain size [5,6]. On the other hand, subsequent passes are regarded as a means to obtain homogeneously-distributed grains of high angle grain boundaries [16]. Multi-pass ECAP process is essential if the strengthening mechanism depends solely on grain refinement through deformation [6]. However, in the case of age-hardenable alloys, ECAP and age-hardening should be considered together. Different approaches were proposed for the optimization of these two strengthening mechanisms, (i.e. grain-size reduction by deformation and precipitation hardening by aging). For example, pre-ECAP aging, dynamic aging and post-ECAP aging are examples of alternative choices that are carried out in combination with multi-pass or single pass ECAP [17–21].

Table 1
As-received compositions for Al 2024 alloy.

Cu	Mg	Mn	Zn	Si	Ni	Cr	Al
4.900	1.240	0.595	0.156	0.106	< 0.1	< 0.1	Bal.

If the pre-ECAP aging is considered, previous studies showed that over-aged 2024 Al alloy subjected to multi-pass ECAP holds a maximum hardness of 187 HV after 3 passes at 150 °C, and further ECAP process results in a hardness drop [17]. The observed ΔH values were high which may be caused by overaging and dynamic recrystallization. Dynamic precipitation is much more promising in terms of hardness enhancement. Kim et al. [18] showed a remarkable increase in strength on Al 6061 after four ECAP passes at 100 °C, but a minimum ΔH of only 15 was obtained.

When multi-pass ECAP is considered, post-ECAP aging becomes less effective for both homogenization and strengthening. This is mainly because ECAP stimulates precipitation due to the high quantity of nucleation sites on which precipitation becomes energetically favorable. Post-ECAP aging after a single pass has led to a hardness of 205 HV after 30 h of aging at 100 °C, but homogeneity-correlated properties are not so clear [20]. Post-ECAP aging is promising for homogenization, which is an outcome of the fine distribution of precipitates nucleated on defects developed during deformation [21]. Several hypotheses [6,10,18] have been proposed to correlate strengthening in age-hardenable ECAPed alloys through grain size refinement by deformation and precipitation hardening by aging; yet, there is no commonly accepted explanation for the exact mechanism.

In this study, two groups of 2024 Al alloy were treated such that the first group of alloys were aged, and the second group was initially processed with one-pass ECAP at high and low back pressures and aged subsequently. The relation between aging time and hardness was investigated. Inhomogeneity after ECAP and the homogenization through aging afterwards were perceived via microhardness maps. OIM images were consulted for further understanding of ECAP deformations in different regions of the sample. Transmission electron microscopy (TEM) images were used to observe the deformed microstructure of ECAPed Al 2024, as well as the precipitation behavior of both solutionized and ECAPed Al 2024.

2. Experimental procedure

The commercial Al 2024 alloy with nominal compositions given in Table 1 was received in rod and rectangular shapes. All specimens were solutionized for 1 h at 495 ± 2 °C in a muffle furnace, quenched in a salt-water-ice mixture of 0 °C, and kept at −18 °C. The rectangular specimens were aged at 190 ± 1 °C up to 18 h without a pre-ECAP process. Rod shaped specimens were

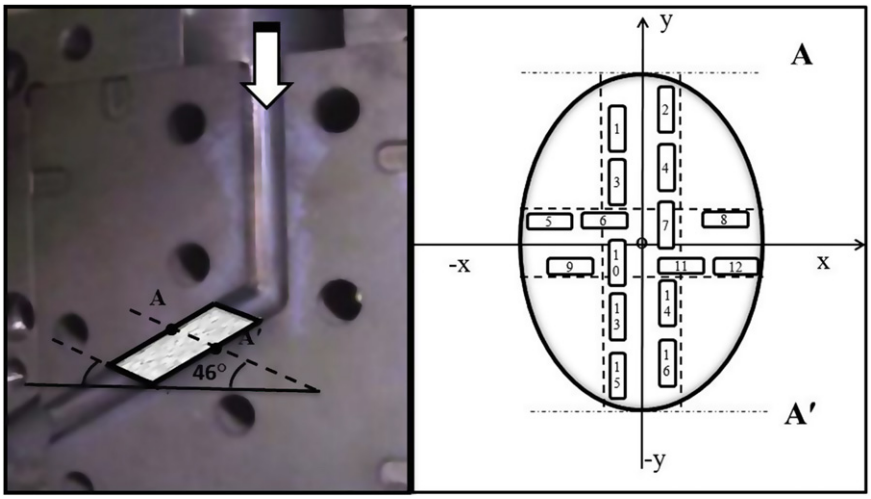

Fig. 1. (a) The 120° ECAP de with a representative sample passing through at a shear angle of 46°. The characterization studies were carried out along the AA′ section shown (left). (b) The sample was separated into 16 regions by locating multiple guide lines as shown, two of which are passing through the center, represented as (*x*,*y*) coordinate system (right).

subjected to ECAP before aging. ECAP was performed at room temperature using an H13 steel die with two channels intersecting at an internal angle of 120° as shown in Fig. 1.

60 mm long Cu blocks were fed into the channel before the sample in order to maintain low and high back pressure. Between each sample and Cu block, cylindrical MoS_2 pellets 5 mm in length were introduced for lubrication. ECAPed samples were kept at −18 °C, as well. After the ECAP process, specimens were subjected to an interrupted aging process at 190 ± 1 °C untill over-aging. Precision cutting was performed from the central region at a shearing plane angle (46°) inclination relative to horizontal, as indicated in Fig. 1, to observe deformation bands in pure shear [16].

The surfaces of the ECAPed and aged specimen were polished, and the high back pressure (HBP) ECAPed sample was marked by microhardness indenter to create guidelines in vertical and horizontal directions across the center for accurate monitoring of the regions during interrupted aging. The aging interruption at 190 °C was performed in 5 min intervals up to 50 min and progressively continued with 60, 65, 75 and 180 min. During each interruption two TEM samples were punched; and a systematic hardness profile was collected. The sample was sub-divided into 16 regions of interest close to the central part as shown in Fig. 1. The central point was assigned as the origin (0,0) of an (x,y) coordinate system, and each hardness indentation was recorded with its relevant coordinate. The hardness penetration results indentations of 60–70 μm in size, therefore a minimum 500 μm interval between each hardness mark (x,y) was kept to maintain data reliability. For each aging time 16 indentations were executed under a constant load of 4.9 N and 10 s of dwell time. The variation in hardness values throughout the cross-sectional area was represented using color-coded contour maps.

Microstructural investigations throughout the shear direction in ECAPed specimens were performed by an electron back-scattered diffraction (EBSD) camera attached to a field-emission gun scanning electron microscope. Specimens for EBSD analyses were prepared using electropolishing with a 5% perchloric acid–ethanol mixture at 20 V. For TEM investigations, selected specimens were further thinned and electropolished in a 25% nitric acid +75% methanol solution at −30 °C until perforation.

3. Results and discussion

The microhardness data in Figs. 2 and 3 show the aging characteristics of solutionized and ECAPed Al 2024. Solution heat-treated specimens with an increase in hardness ~50% up to 148 HV show a common aging behavior with Al 2024 series aluminum.

The Guinier–Preston–Bagaryatsky zone (GPB)-S″ peak is observed at about 5.5 h before peak aging, the formation of S′ at 11.5 h. This

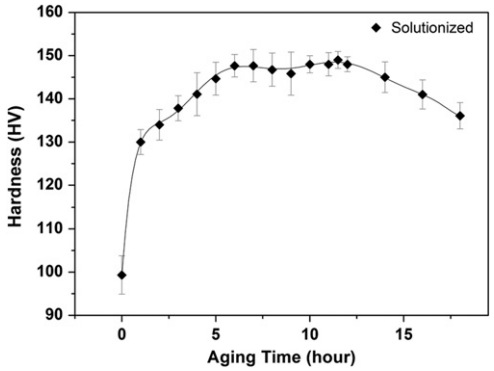

Fig. 2. Aging behavior of Al 2024 at 190 °C after quenching the sample, 1 h solutionized at 495 °C, into 0 °C ice–salt–water mixture. The peak aging is observed at 11.5 h.

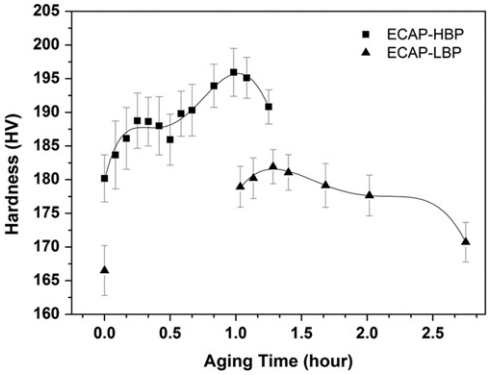

Fig. 3. Aging behaviors of ECAP processed samples with low back pressure (LBP) and high back pressure (HBP) at an aging temperature of 190 °C.

shows a slight variation from the 12 h peak aging time and is probably due to differences in alloying quantity. The aging behavior of ECAPed specimens (Figs. 2, 3) is dramatically different as compared to solutionized specimens. The maximum attainable hardness values increased considerably, and the time period required reaching peak age condition decreased after the ECAP process. The hardness values obtained for high back-pressure ECAP are higher as compared to low back-pressure process. Accordingly, for homogenization and microstructural analyses high back-pressured ECAP specimens were selected for comparison with solutionized alloys.

The homogenization in hardness for solution heat treated Al 2024 alloys is observed at periods slightly over 11.5 h corresponding to over aging. The standard deviation in this regime drops to 1.71 HV as compared to 4.02 HV for the solution heat-treated condition. If the hardness inhomogeneity index is considered, H_i becomes as 0.14 and 0.04 for solution heat-treated and over-aged conditions, respectively. On the other hand, homogenization of hardness variation in ECAPed specimens starts around 195 HV with a standard deviation of 3.03 HV. The standard deviation seems high as compared to solution heat treated specimens; however, when the hardness inhomogeneity index is taken into account there is a notable decrease. H_i values before and after aging in ECAPed specimens are 0.083 and 0.046, respectively. As mentioned previously, a common belief regarding ECAP is that the deformation inhomogeneity after the first pass is considerably higher, and subsequent passes are required to reach the desired homogeneity [5]. However, the results of this study have shown that deformation inhomogeneity, relatively similar to the solution heat treated condition, can be obtained after a single pass ECAP using age-hardenable Al 2024. In common ECAP process, the first pass ensures the maximum increase in strength, and the following passes provide the homogeneity and refinement of microstructure. In that sense, the results of the current study are remarkable since relatively high hardness and homogenization levels are obtained after a single pass ECAP for Al 2024 alloys. Therefore, it is worth investigating the underlying mechanism in single pass ECAP for an age-hardenable alloy system.

ECAP causes different levels of deformation in various parts of the specimen. This can be easily observed from the OIM images taken at the top, center, and bottom regions of the specimen. Fig. 4(a) shows the OIM image from the ECAPed specimen before the aging process, indicating randomly oriented equiaxed grains. After a single-pass ECAP process, the level of texture is higher in the top and bottom part of the specimen as compared to the central region. On the other hand, grain refinement is mostly observed in the central region.

Fig. 5 shows the spatial distribution of hardness with respect to aging in deformed specimens after ECAP processing. The specimen before the aging process shows regions with different

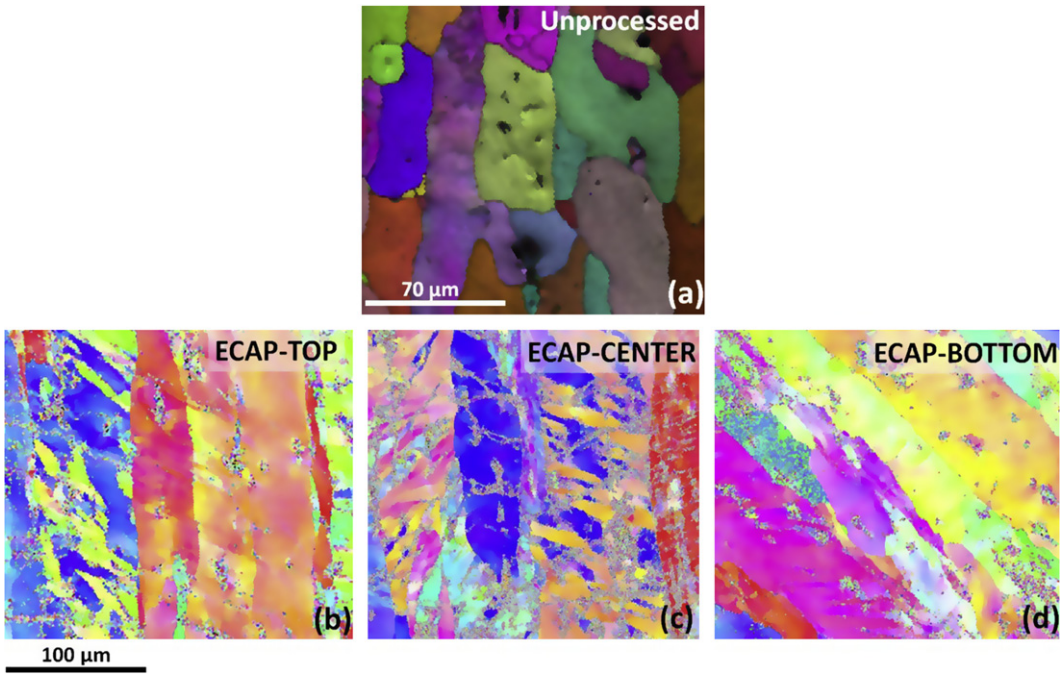

Fig. 4. OIM images of (a) solutionized Al 2024, (b) top, (c) center, (d) bottom parts of ECAPed Al 2024 sample. The grain refinement is maximized at the center of the sample whereas elongated grains are viewed in b, c and d.

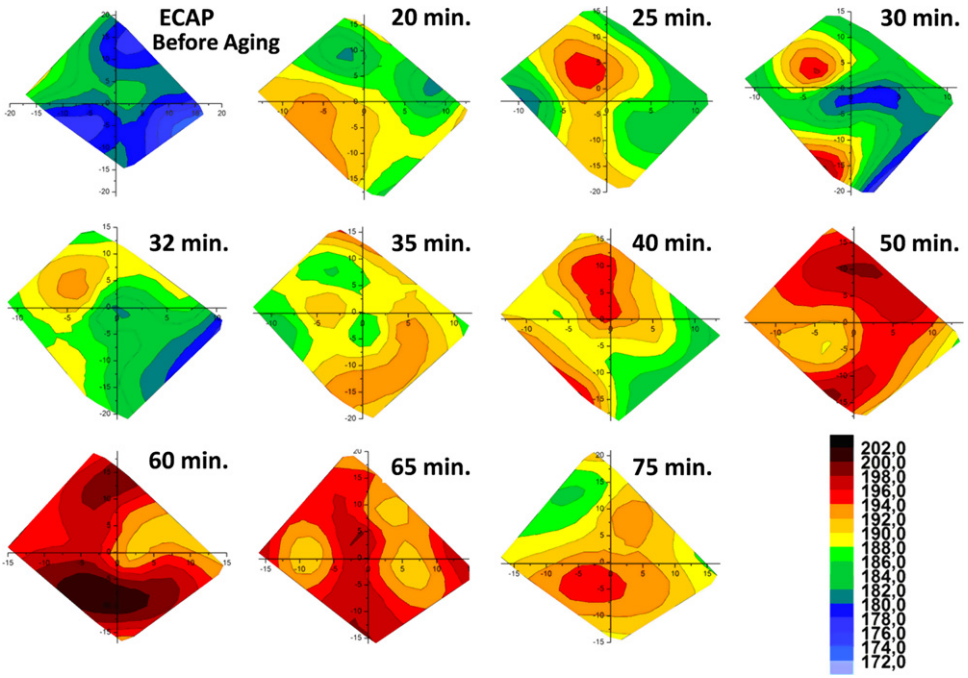

Fig. 5. The hardness contour maps for high back pressure ECAP processed Al 2024. The aging leads to precipitation sequence with a peak of S″/GPB at 30 min and a peak of S/S′ at 60 min.

hardness values corresponding to a H_i value of 0.083. The highest hardness is at the center where pure shear is more effective and the lowest value at the bottom; this is also in good agreement with finite element studies on the corner gap effect in ECAP [12,13], as the corner angle used in this study is below 45°. Up to 20 min of aging, no prominent change in hardness is observed; however, the region at the upper part of the specimen subsequently starts to age-harden. The maps for 25 and 30 min confirm the S″ precipitation. The peak hardness is reached after 60 min of aging. Consecutive aging does not cause any further increase in the overall hardness; rather, it results in a homogenous distribution. At 65 min of aging a hardness inhomogeneity index of 0.046 is obtained, as shown in Fig. 6. This value is close to that of the most homogeneous non-ECAPed Al 2024 age-hardened alloy and it is even better than multi-pass ECAPed pure Al with a hardness inhomogeneity index of 0.093 [14].

Such a low hardness inhomogeneity index may seem surprising after an ECAP process with a single pass run. The major strengthening mechanism in ECAP is grain size refinement through severe plastic deformation and several studies [5,6] have shown that

multiple passes are required to reach a successful evolution of the microstructural integrity and thus a good level of hardness homogeneity along the cross-sectional regions. However, it should be noted that the material processed in this study is an age-hardenable alloy. Therefore, together with the microstructural refinement, precipitation hardening should also be considered.

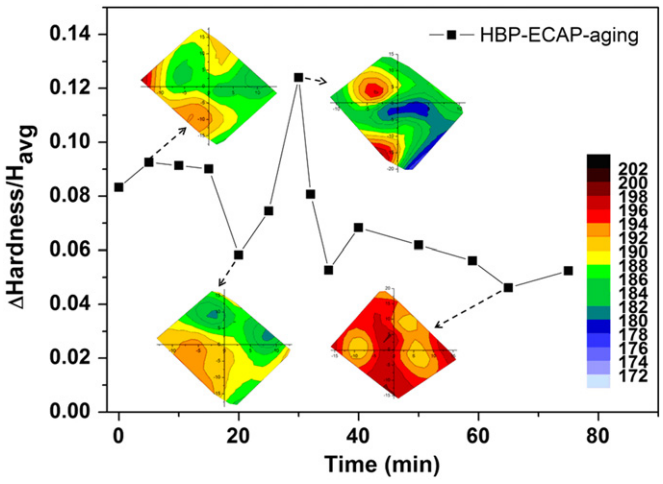

Fig. 6. Hardness inhomogeneity index ($H_i = \Delta H/H_{avg}$) variations in (HBP-high back pressure) ECAPed sample throughout aging at 190 °C. The corresponding hardness contour maps in Fig. 5 are reprinted for 5 min, 20 min, 30 min and 65 min. Maximum homogeneity is observed for 65 min of aging.

Fig. 7 shows the TEM micrographs for solutionized + aged, ECAPed, and ECAPed + aged specimens. The specimens solutionized and aged for 11.5 h to reach the maximum hardness (peak aging) consist of S′ (Al_2CuMg) precipitates and T-phase ($Al_{20}Cu_2Mn_3$) dispersoids on the Al matrix. The dispersoids are believed to form during solidification [1], and the S′ phase originates from the expected precipitation sequence in age-hardenable Al–Cu–Mg alloy [22]. Bright (BF) and dark (DF) field analyses have shown that S′ precipitates are needle-like in morphology and elongated to $\langle 001 \rangle_{Al}$ crystallographic direction. Their average length is on the order of 400 nm. TEM analyses of ECAPed specimens before aging are in good agreement with EBSD analyses. BF images indicate elongated Al grains and T-phase dispersoids. Since these alloys are not age-hardened no precipitate formation is detected. One interesting observation is the formation of dislocation clusters after the ECAP process. These clusters form networks within the Al matrix, and they were routinely observed in TEM specimens prepared from various regions of the ECAPed sample [Fig. 7(c) and (d)]. Such dislocation networks refer to the formation of subgrains due to severe plastic deformation [23] during the ECAP process. Mainly due to size restrictions, these subgrains cannot be observed in EBSD analyses. Age-hardening of the ECAPed samples results in the formation of highly populated and randomly distributed S′ precipitates, as shown by BF and DF images in Fig. 7(e) and (f). The average size of the precipitates is ~30–40 nm after the aging of ECAP specimens. These precipitates are considerably smaller as compared

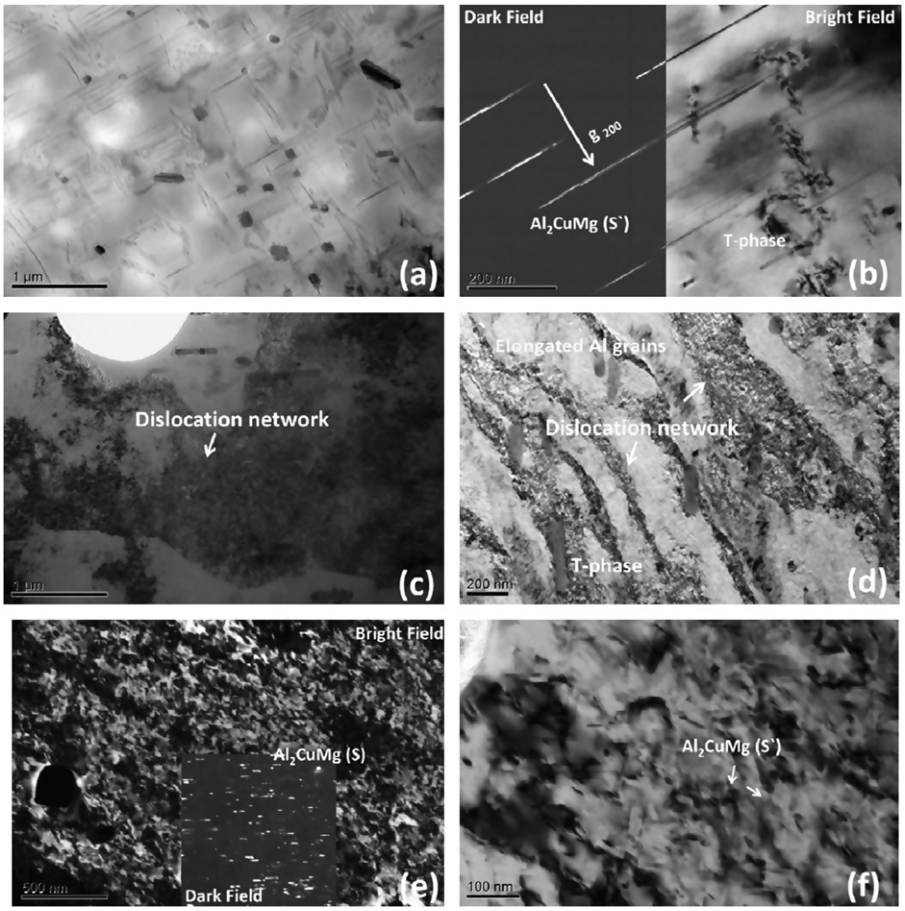

Fig. 7. (a) and (b) Bright field (BF) and dark field (DF) images of solutionized +11.5 h aged Al2024 showing the S′ precipitates in needle form and T phase dispersoid ($Al_{20}Cu_2Mn_3$) as large particles (c) and (d) BF images of single pass ECAPed Al 2024 with dislocation network and T-phase dispersoids. (e) BF and DF images of ECAPed + aged (65 min at 190 °C) Al 2024 showing S′ precipitates finely distributed in the dislocation network, (f) BF of ECAPed + aged (65 min at 190 °C) Al 2024 showing the fine size of Al_2CuMg (S′) precipitates.

to the unprocessed condition. Previous studies have shown that dislocation networks can act as potent nucleation sites for the formation of S′ precipitates within the subgrains [20]. This explains the early achievement of peak hardness for ECAPed specimens as compared to unprocessed specimens upon aging. In the case of ECAP, the S′ precipitates can heterogeneously nucleate on the sites created by dislocations. Moreover, it seems that the number density of dislocations play an important role in determining the population of S′ precipitates. The number density of dislocation clusters increases considerably after the ECAP [Fig. 7(c)], and so does the number of S′ precipitates [Fig. 7(e)]. The average size of these precipitates is much smaller than in the unprocessed alloy [Fig. 7(b)]. This is probably controlled by the size of the sub-grains created by dislocations. Perhaps the most intriguing observation is the random distribution of the S′ precipitates in ECAPed specimen after aging. Various parts of the specimen were investigated at peak hardened conditions using TEM, and these precipitates were found to exist together with the dislocation clusters. This may explain the low inhomogeneity index calculated for peak-aged specimens after the ECAP process. The single pass ECAP process is not effective for increasing strength by creating a homogeneous microstructural refinement as in a conventional multi-pass process (Fig. 4). Moreover, aging of these alloys results in recrystallization and recovery of new strain free grains. On the other hand, a single pass run is effective for creating dislocation clusters throughout the specimens. Upon aging to maximum peak hardness S′ precipitates nucleate and grow on these sites concurrently, resulting in a high degree of hardness homogeneity on the cross-sectional profiles. Accordingly, it can be concluded that single pass ECAP processing does not lead to strengthening by forming homogeneously-distributed ultra-fine grain structure but rather creating networks of dislocation clusters, which act as nucleation sites for S′ precipitates.

4. Conclusions

1. Single pass ECAP results in an inhomogeneous microstructure and hardness. OIM images and hardness maps show that the center is the most effectively ECAPed region compared to upper and lower parts mostly due to corner gap.
2. Hardness results show that ECAP has a profound effect on the aging time of Al 2024. The peak aging time at 190 °C was found to decrease from 11.5 to 1 h after a single pass ECAP process. Homogenization of single pass ECAPed Al 2024 is achieved followed by 65 min of aging at 190 °C; 195 HV hardness with a hardness inhomogeneity index (H_i) of 0.046 was accomplished approximating the 0.04 of the solutionized and aged counterpart.
3. TEM images show that average precipitate size decreased from 400 nm down to 30–40 nm in ECAPed Al 2024 as compared to solutionized specimens. The precipitation is specifically observed in regions of the dislocation network, and the size limitation is compatible with the cells formed in this network. Thus, the homogenization can be attributed to precipitation hardening due to very fine and well distributed precipitates.

References

[1] J.R. Davis, ASM Specialty Handbook: Aluminum and Aluminum Alloys, ASM International, Materials Park, 1996.
[2] J.C. Williams, E.A. Starke Jr., Acta Mater. 51 (2003) 5775–5799.
[3] S.M. Kumaran, Mater. Sci. Eng. A 528 (2011) 4152–4158.
[4] G.F. Dieter, Mechanical Metallurgy, third ed., McGraw Hill, New York, 1986.
[5] R.Z. Valiev, R.K. Islamgaliev, I.V. Alexandrov, Prog. Mater. Sci. 45 (2000) 103–189.
[6] R.Z. Valiev, T.G. Langdon, Prog. Mater. Sci. 51 (2006) 881–981.
[7] Z. Horita, T. Fujinami, T.G. Langdon, Mater. Sci. Eng. A 318 (2001) 34–41.
[8] Z. Horita, T.G. Langdon, Scr. Mater. 58 (2008) 1029–1032.
[9] R. Vafaeia, M.R. Toroghinejada, R. Pippanbring, Mater. Sci. Eng. A 536 (2012) 73–81.
[10] X.G. Qiao, M.J. Starink, N. Gao, Mater. Sci. Eng. A 513–514 (2009) 52–58.
[11] M. Prell, C. Xu, T.G. Langdon, Mater. Sci. Eng. A 480 (2008) 449–455.
[12] A.V. Nagasekhar, H.S. Kim, Comp. Mater. Sci. 43 (2008) 1069–1073.
[13] S.C. Yoon, H.S. Kim, Mater. Sci. Eng. A 490 (2008) 438–444.
[14] F. Djavanroodi, M. Daneshtalab, M. Ebrahimi, Mater. Sci. Eng. A 535 (2012) 115–121.
[15] V.P. Basavaraj, U. Chakkingal, T.S.P. Kumar, J. Mater. Proc. Technol. 209 (2009) 89–95.
[16] C. Xu, Z. Horita, T.G. Langdon, Mater. Sci. Eng. A 318 (2001) 34–41.
[17] Y.W. Ma, J. Woo, Mater. Sci. Eng. A 529 (2011) 1–8.
[18] M. Vaseghi, A.K. Taheri, S.I. Hong, H.S. Kim, Mater. Des. 31 (2010) 4076–4082.
[19] X.G. Qiao, M.J. Starink, N. Gao, Mater. Sci. Eng. A 513–514 (2009) 52–58.
[20] W.J. Kim, C.S. Chung, D.S. Ma, S.I. Hong, H.K. Kim, Scr. Mater. 49 (2003) 333–338.
[21] E. Saraloglu, E. Tan, C.H. Gur, Steel Res. Int. (2008) 467–471.
[22] T.S. Parel, S.C. Wang, M.J. Starink, Mater. Des. 31 (2010) S2–S5.
[23] Y. Estrin, L.S. Toth, A. Molinari, Y. Breachet, Acta Mater. V46 (15) (1998) 5509–5522.